

Article

An NIR Emissive Donor- π -Acceptor Dicyanomethylene-4H-Pyran Derivative as a Fluorescent Chemosensor System towards Copper (II) Detection

Agata Karkosik and Artur J. Moro * 

LAQV-REQUIMTE, Departamento de Química, CQFB, Universidade Nova de Lisboa, Monte de Caparica, 2829-516 Caparica, Portugal

* Correspondence: artur.moro@fct.unl.pt

Abstract: A novel donor- π -acceptor fluorescent dye as a chemosensor for Cu^{2+} ions is herein presented. The fluorophoric core consists of a 3,5-diphenyl-dicyanomethylene-4H-pyran (DCM), with extended styryl chains on positions 2 and 6, bearing terminal di-(2-picolyl)amine (DPA) groups for metal coordination. Optical characterization of the chemosensor dye reveals an absorption maximum at ca. 500 nm and a strong bathochromic shift in the emission, reaching ca. 750 nm in polar solvents. This solvatochromic behavior, which yields very large Stokes shifts (up to $\sim 6700 \text{ cm}^{-1}$), is characteristic of the strong intramolecular Charge Transfer (CT) nature of this chromophoric system. While the chemosensor has demonstrated no changes in its optical properties over a wide pH range (2–12), a strong quenching effect was observed upon Cu^{2+} coordination, with a 1:1 binding stoichiometry, indicating that only one DPA unit is capable of effectively chelating Cu^{2+} , rendering the second DPA motif inactive. The binding constant was determined to be $7.5 \times 10^7 \text{ M}^{-1}$, indicating a very high sensitivity, and an LOD of 90.1 nM. Competition assays have demonstrated that the chemosensor is highly selective towards Cu^{2+} , even in the presence of excesses of other mono- and di-valent cations. Co^{2+} and Ni^{2+} proved to be the strongest interferents, particularly in the luminescent response. Paper test-strips prepared with the embedded sensor showed a fluorometric response in the presence of different copper (II) concentrations, which attested to the potential of this chemosensor to be used in the determination of Cu^{2+} content in aqueous media, for in-field applications.

Keywords: Di-(2-picolyl)amine (DPA); copper (II); fluorescent sensor; 3,5-diphenyl-dicyanomethylene-4H-pyran (DCM); near-infrared (NIR); charge transfer (CT)



Citation: Karkosik, A.; Moro, A.J. An NIR Emissive Donor- π -Acceptor Dicyanomethylene-4H-Pyran Derivative as a Fluorescent Chemosensor System towards Copper (II) Detection. *Chemosensors* **2022**, *10*, 343. <https://doi.org/10.3390/chemosensors10080343>

Academic Editor: Guo-Hui Pan

Received: 19 July 2022

Accepted: 17 August 2022

Published: 22 August 2022

Publisher's Note: MDPI stays neutral with regard to jurisdictional claims in published maps and institutional affiliations.



Copyright: © 2022 by the authors. Licensee MDPI, Basel, Switzerland. This article is an open access article distributed under the terms and conditions of the Creative Commons Attribution (CC BY) license (<https://creativecommons.org/licenses/by/4.0/>).

1. Introduction

Fluorescent chemosensors have been widely investigated over the past few decades, mainly due to their high sensitivity when compared to other sensor systems, allowing for a high spatiotemporal resolution and continuous monitoring of analyzed samples [1]. Sensors that are coupled to metal binding moieties have been designed since the early 1980s, and an enormous collection of molecules has been reported, where the chelating moiety plays the key role in the selectivity towards a specific metal cation [2]. A particular successful case is the di-(2-picolyl)-amine (DPA) chelating group, which has been thoroughly investigated by a large number of research groups.

The development of new sensor systems for specific metal ions has been boosted by the relevance of several cations, given their roles in biological processes, and in some cases, their inherent toxicity for the environment. Along with iron and zinc, copper plays a key role as a catalytic cofactor for many metalloenzymes in the human body. It is therefore an essential trace element for both fauna and flora [3]. Nevertheless, at certain concentrations, it is toxic to fish and aquatic life due to high levels of bioaccumulation and its integration within the food chain, and long-term exposure can lead to severe food poisoning, ultimately resulting in permanent damage to the liver and kidneys. Additionally, it has been linked to

several neurodegenerative diseases (e.g., Alzheimer's and Wilson's diseases), probably due to its involvement in the production of reactive oxygen species [4–6].

DPA-based sensors for Cu^{2+} with several different fluorophores have been reported, including ruthenium (II) [7,8] and iridium (II) [9] complexes, naphthalimide [10–12], chalcones [13] and BODIPY dyes [14,15], among others [16].

Over recent years, significant research effort from the scientific community has been directed to designing chemosensors with optical properties in the near-infrared (NIR) region, i.e., with absorption and emission above 700 nm. This specific class of sensors is particularly relevant for biological samples, since it is in this spectral region that light can penetrate deeper into cellular tissues, thereby allowing in vivo monitoring with minimal radiation damage [17]. Another significant advantage for optical sensors operating in the NIR region is the minimum fluorescence background, and another is less light scattering with visible light, especially for cases where less intrusive integration of artificial lighting may be better suited [18]. While several NIR systems are known to preferentially detect copper (II), to the best of our knowledge, only one integrates DPA as a Cu^{2+} -selective coordination moiety [19].

Dicyanomethylene-4*H*-pyran (DCM) fluorophores have been reported to absorb and/or emit NIR light, since they present a strong intramolecular Charge Transfer (CT) character which shifts the optical properties towards lower energies in polar media, due to the strong stabilization of the excited CT state [20,21]. Additionally, extension of the π -conjugated chain is readily accessible through Knoevenagel condensation of the end methyl groups with aldehyde derivatives, resulting in a red shift of the optical properties of the DCM core [22,23].

With this in mind, we designed a NIR fluorescent chemosensor with a 3,5-diphenyl-dicyanomethylene-4*H*-pyran (DCM) core, with an extended push-pull π -system, possessing two DPA units for metal ion detection, and fully characterized it in terms of sensitivity and selectivity towards metal ions, both in solution and in paper-support.

2. Materials and Methods

2.1. Synthesis

All used chemicals were of analytical grade and used as purchased. Fine chemicals were acquired from Sigma-Aldrich (St. Louis, MO, USA), and solvents were purchased either from Sigma-Aldrich or Carlo Erba (Barcelona, Spain).

2.1.1. Synthesis of 2,6-dimethyl-3,5-diphenyl-4*H*-pyran-4-one (1)

1,3-Diphenylpropan-2-one (2.14 g, 10.0 mmol) and acetic anhydride (20 mL) were added to a 50 mL round-bottom flask. After 1,3-diphenylpropan-2-one was fully dissolved under stirring conditions, polyphosphoric acid (PPA) (6.75 g, 20.0 mmol) was added to the flask. The reaction mixture was stirred at 140 °C for 12 h. The reaction mixture was cooled to room temperature and then poured into 200 mL of water. The mixture was then extracted with CH_2Cl_2 , and the combined organic phases were dried with anhydrous Na_2SO_4 . The solution was filtered, and the organic solvent was removed under reduced pressure and passed through a silica gel column, with dichloromethane as the solvent, to give a light yellow solid (1) (0.704 g, 28.9% yield). ^1H NMR (400 MHz, CDCl_3) δ : 7.41 (t, $J = 7.4$ Hz, 4H), 7.35 (d, $J = 7.1$ Hz, 2H), 7.30 (d, $J = 7.4$ Hz, 4H), 2.28 (s, 6H). ^{13}C NMR (101 MHz, CDCl_3) δ : 176.81, 161.71, 132.83, 130.37, 128.16, 127.68, 126.45, 18.78.

2.1.2. Synthesis of 2-(2,6-dimethyl-3,5-diphenyl-4*H*-pyran-4-ylidene) Malononitrile (2)

Compound 1 (0.704 g, 2.55 mmol) and acetic anhydride (5 mL) were added to a 250 mL round-bottom flask. After compound 1 was fully dissolved under stirring conditions, malononitrile (2.64 g, 5.92 mmol) was added and the reaction mixture was stirred at 140 °C for 24 h. Afterwards, it was cooled to room temperature, and then we poured in 35 mL of water. The mixture was then extracted with CH_2Cl_2 , and the organic phase was dried with anhydrous Na_2SO_4 . We filtered it, and the solvent was removed under reduced

pressure. The residue was purified through a silica gel column, using petroleum ether:ethyl acetate (5:1), to yield a light red solid (2) (0.264 g, 31.8% yield). ^1H NMR (400 MHz, CDCl_3) δ : 7.55–7.47 (m, 6H), 7.33–7.28* (m, 4H), 2.10 (s, 6H). ^{13}C NMR (101 MHz, CDCl_3) δ : 158.98, 153.54, 133.63, 130.95, 129.81, 129.24, 120.79, 114.88, 63.41, 18.96.

*Integration was mixed with that of CDCl_3 .

2.1.3. Synthesis of 2-(2,6-bis((E)-4-((2-(bis(pyridin-2-ylmethyl)amino)ethyl)(methyl)amino)styryl)-3,5-diphenyl-4H-pyran-4-ylidene)malononitrile (4)

4-((2-(Bis(pyridin-2-ylmethyl)amino)ethyl)(methyl)amino)benzaldehyde (3) (0.14 g, 0.39 mmol), acetonitrile (5 mL), compound 2 (0.324 g, 0.20 mmol) and piperidine (0.5 mL) were added to a round-bottom flask. The mixture was stirred at 80 °C for 10 h. After the reaction mixture was cooled to room temperature, the solvent was removed under reduced pressure. The residue was passed through a silica gel column, with dichloromethane as a starting solvent. After collecting all impurities, the solvent was switched to dichloromethane:methanol:ammonia (9.5:0.5:0.01). Upon evaporation of the solvents, a red solid was collected (4) (0.075 g, 37.7% yield). ^1H NMR (400 MHz, CDCl_3) δ : 8.53 (d, $J = 4.9$ Hz, 2H), 7.61 (t, $J = 7.8$ Hz, 2H), 7.58–7.50 (m, 3H), 7.47–7.35 (m, 5H), 7.18–7.09 (m, 4H), 6.48 (d, $J = 8.5$ Hz, 2H), 6.23 (d, $J = 15.8$ Hz, 1H), 3.89 (s, 4H), 3.48 (t, $J = 7.1$ Hz, 2H), 2.89 (s, 3H), 2.76 (t, $J = 7.2$ Hz, 2H). ^{13}C NMR (101 MHz, CDCl_3) δ : 159.16, 155.13, 153.56, 150.27, 149.13, 137.26, 136.47, 133.67, 131.96, 129.67, 129.44, 129.01, 123.02, 122.97, 122.17, 119.20, 116.06, 112.71, 111.60, 60.97, 50.65, 50.47, 38.64.

2.2. UV-Vis and Fluorescence Measurements

Absorption spectra were acquired on a Varian Cary 100 Bio UV-Vis spectrophotometer (Agilent, Santa Clara, CA, USA). Emission spectra were obtained using a Horiba–Jobin–Yvon SPEX Fluorolog 3.22 spectrofluorometer (HORIBA, Kyoto, Japan). Solutions for UV-Vis absorption and fluorescence measurements were prepared by adding an aliquot of 57 μL of a 1.32×10^{-4} M methanolic solution of 4, 1470 μL of methanol and 1500 μL of buffer, for a final chemosensor concentration of 2.5 μM . For all metal titrations, 10 mM HEPES buffer at $\text{pH} 7.0 \pm 0.2$ was used. pH titrations were performed using Theorell and Stenhagen universal buffer [24]. Metal ion titrations were performed by adding small aliquots of a metal stock solution to a cuvette containing solely the chemosensor, recording both UV-Vis and luminescence spectra in between additions. Posterior correction on the values of chemosensor and metal concentrations to account for the volume change upon each addition were made. The limit of detection (LOD) of Cu^{2+} was determined according to IUPAC guidelines [25], by measuring seven independently prepared samples of chemosensor 4 with no metal (blank) and applying the formula: $\text{LOD} = |3\sigma/b|$, where σ represents the standard deviation of these measurements, and b represents the slope over a fixed linear range (0–1.4 μM of Cu^{2+} was selected). All UV-Vis absorption and emission spectra were acquired in 1 cm Plastibrand cuvettes on a Varian Cary 100 Bio U-spectrophotometer, except for experiments with different organic solvents, where a 1 cm quartz cuvette was used. Fluorescence quantum yield for 4 was determined using 4-(dicyanomethylene)-2-methyl-6-(p-dimethylaminostyryl)-4H-pyran ($\phi_f = 0.43$ in methanol) [26]. The binding constants for 4- Cu^{2+} and 4- Co^{2+} were determined by fitting the experimental data to a Henderson-Hasselbalch binding model using the Solver Add-In from Microsoft Excel [27]. Paper test-strips were prepared by incubating 1 by 2 cm paper rectangles (FILTER-LAB[®] medium-filtration qualitative filter paper from Anovia, Barcelona, España) for 30 min in a 0.5 mM methanolic solution of chemosensor 4. Afterwards, the paper was air dried, dipped in aqueous solutions of different copper (II) concentrations and left to dry once more before recording the photos (ambient light and 365 nm UV light) with an iPhone SE 2020 (Apple, Cupertino, CA, USA), and acquiring the luminescent spectra.

3. Results and Discussion

3.1. Synthesis

The synthetic design of chemosensor **4** comprised a total of three reaction steps (Figure 1). The core dicyanomethylene-4*H*-pyran was obtained by reacting 1,3-diphenylpropan-2-one with acetic anhydride, under acidic conditions, followed by the addition of malonitrile at position 4 [23].

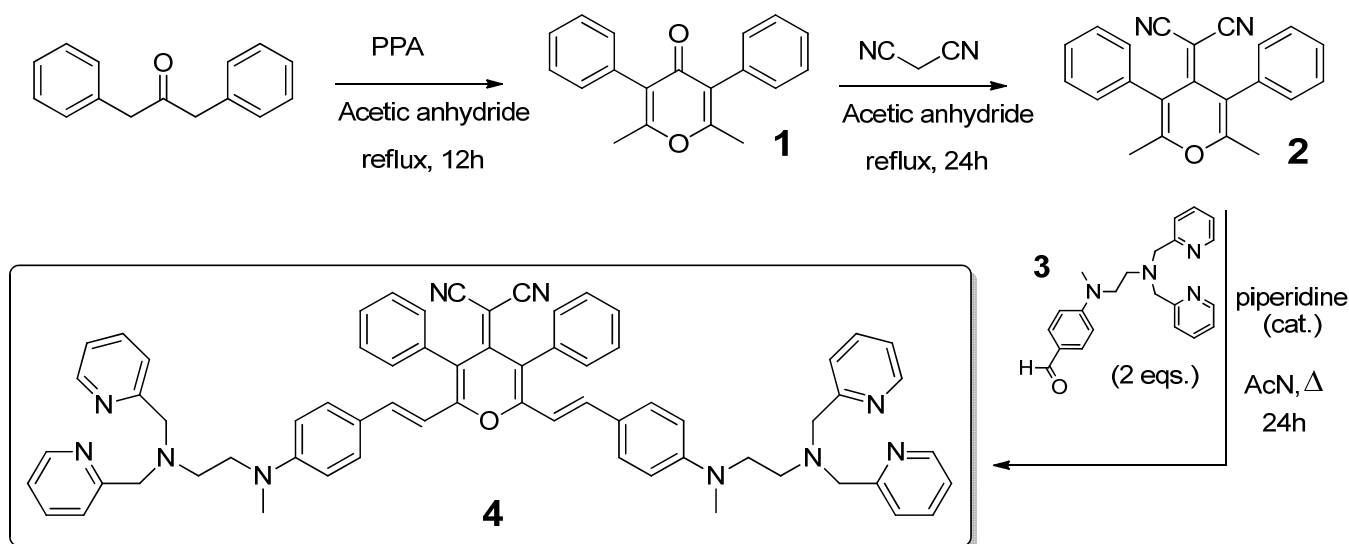


Figure 1. Full synthesis of chemosensor **4**.

The DPA motif was introduced by reacting 4-((2-(bis(pyridin-2-ylmethyl)amino)ethyl)(methyl)amino)benzaldehyde (**3**) [13] with compound **2**, via a Knoevenagel condensation, to yield the final chemosensor **4**. Full NMR and HRMS spectra for structural characterization of **4** can be found in the Supporting Information (Figures S1–S11).

3.2. Photophysical Characterization

Chemosensor **4** possesses a dicyanomethylene-4*H*-pyran as the core fluorophore. The conjugation of the π -system was extended with the introduction of two styryl “arms”, each with an amine in position 4. The donor character each of these nitrogen’s lone pair of electrons, combined with the electron withdrawing nature of the pyran core, causes a strong push-pull effect, leading to a pronounced red shift in the emission of the fluorophore in highly polar solvents. Indeed, Figure 2 shows the linear relationship between the Stokes shift of **4** and the empirical polarity parameter E_T^N [28] (see Table S2 for the list of used solvents and respective polarity data), which indicates the strong intramolecular Charge Transfer (CT) character of this molecule. In highly polar media, this value reaches up to 6700 cm^{-1} , reaching the NIR region with an emission maximum at ca. 750 nm. This large Stokes shift in polar solvents is accompanied by a strong non-radiative decay from the excited state, which is reflected in the recorded fluorescent quantum yield of 0.008, consistent with molecules undergoing intramolecular CT processes in the excited state [29].

For binding metal cations, the nitrogens from the DPA unit must have lone electron pairs available to act as chelators. Titration of chemosensor **4** showed very low sensitivity over a wide range of pH values (Figure S12), indicating that the protonation of the aliphatic non-conjugated tertiary amine (which is expected to occur at a pH between 5 and 6 [30]) does not reflect in the optical properties of the molecule. The protonation of the nitrogen that is directly coupled to the fluorophore is expected to occur at lower pH values, since its lone pair of electrons acts as a charge donor to the π -conjugated system.

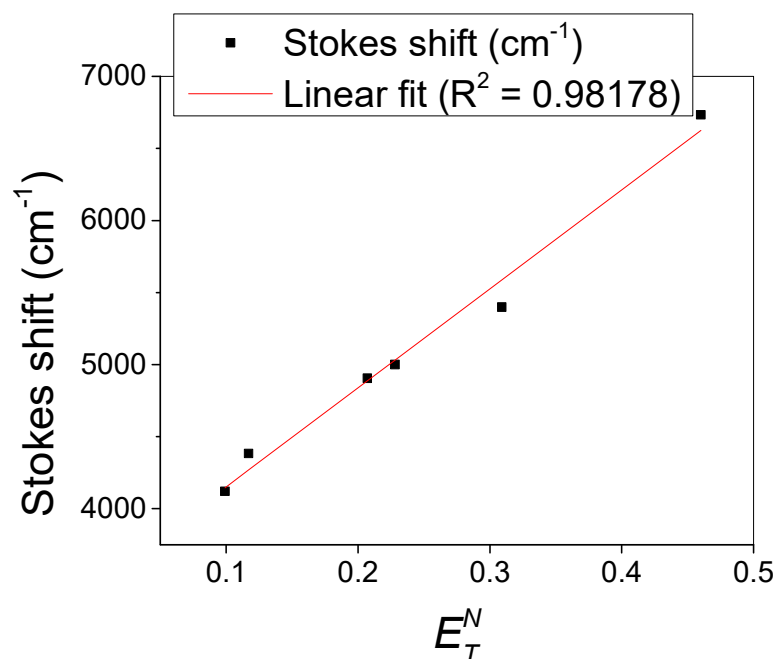


Figure 2. Effect of solvent polarity (E_T^N) on the observed Stokes shift for chemosensor **4** in different solvents (black dots), with the corresponding linear trend (red line).

3.3. Metal Sensitivity/Selectivity

In order to understand the influence of chelation efficiency and how this process affects the optical properties of **4**, its optical properties were measured in the presence of different metal cations. UV-Vis spectra revealed that the chemosensor presented a noticeable selectivity for Cu(II): a strong blue shift of the maximum absorption band from 500 to 450 nm took place. The presence of other cations produced little to no changes in the absorption spectra. Indeed, even with a naked eye, it was possible to see the change in color from red to yellow in the presence of Cu^{2+} . Nevertheless, one could still distinguish a group of five cations, Zn^{2+} , Cd^{2+} , Ni^{2+} , Co^{2+} and Pb^{2+} , that induce slight hypsochromic (≤ 13 nm) and hypochromic shifts of the free chemosensor band (Figure 3), leading to a slight change in the color of **4** from red to orange (Figure S13A).

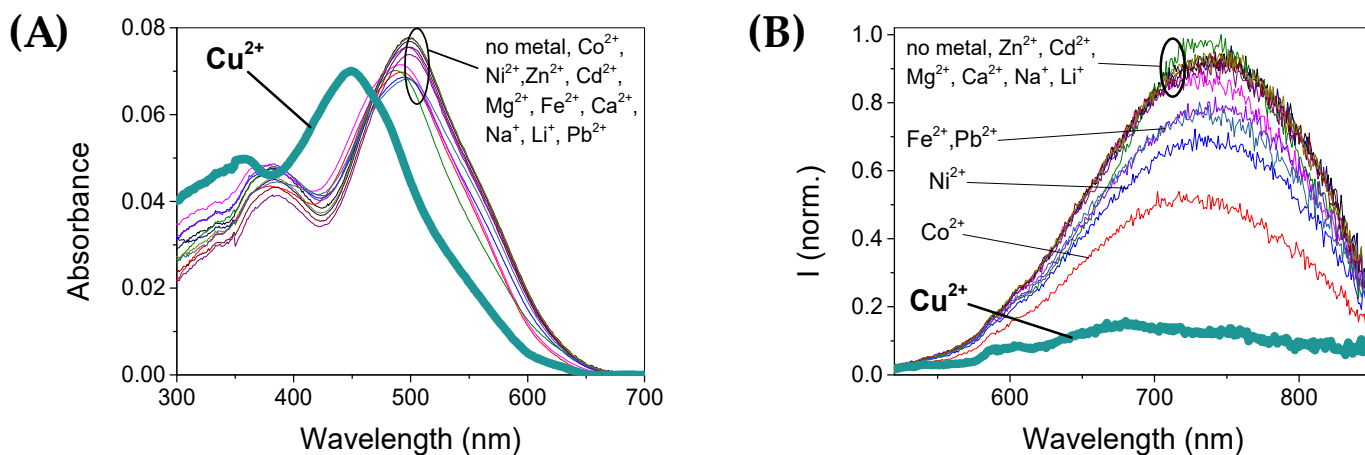


Figure 3. UV-Vis (A) and emission (B) spectra of chemosensor **4** (2.5 μM) in the presence of two equivalents of different metal ions, in a 50:50 mixture of methanol and 0.01 M HEPES buffer at pH = 7.1 ($\lambda_{\text{EXC}} = 500$ nm).

This strong shift from the ground-state absorption spectra to higher energies suggests that the aromatic nitrogen which is directly coupled with the π -conjugated chain of the dicyanomethylene-4*H*-pyran fluorophore also contributes to the coordination sphere for copper chelation (see Figure 5, below). In terms of luminescence, Cu^{2+} was also the metal that prompted the strongest emission changes in **4**. A strong quenching effect was observed upon increasing the concentration of this cation, which was also reflected when looking at solutions of **4** under 365 nm UV light (Figure S13B). However, some quenching effect was also observed with other metals, particularly for Co^{2+} , and to a lesser extent, also Ni^{2+} , Fe^{2+} and Pb^{2+} . Taking a closer look at the behavior of **4** with copper (II), we performed UV-Vis and fluorescence titrations, to understand the sensitivity against this specific metal cation. The results are presented in Figure 4.

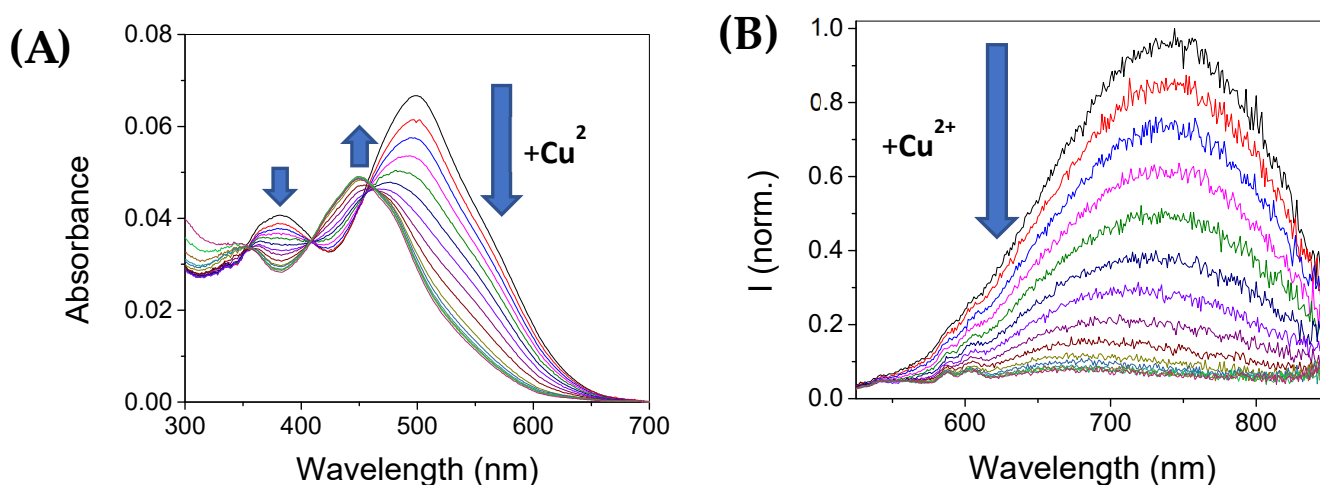


Figure 4. UV-Vis (A) and emission (B) spectra of **4** (2.5 μM) upon addition of increasing amounts of Cu^{2+} , in a 50:50 mixture of methanol and 0.01 M HEPES buffer at pH = 7.1 ($\lambda_{\text{EXC}} = 500 \text{ nm}$).

For the UV-Vis absorption spectra, a decrease in the absorption bands centered at 382 and 500 nm was observed upon increasing Cu^{2+} concentration, along with a simultaneous rise in a new band at circa 450 nm, corresponding to **4**- Cu^{2+} complex. The emission from **4** was also strongly quenched by increasing amounts of Cu^{2+} up to about 1 equivalent, from which point it reached a plateau and remained unchanged (Figure 4B and Figure 6A, below). This trend suggests that, although chemosensor **4** bears two DPA moieties, the binding of a first Cu^{2+} ion influences the conjugated π -system in such a way that binding a second Cu^{2+} is no longer favorable, since the lesser charge density in the central fluorophore displaces the lone pair of electrons of the nitrogen that is located on the opposite side of the molecule, in order to compensate and stabilize the conjugated system (Figure 5).

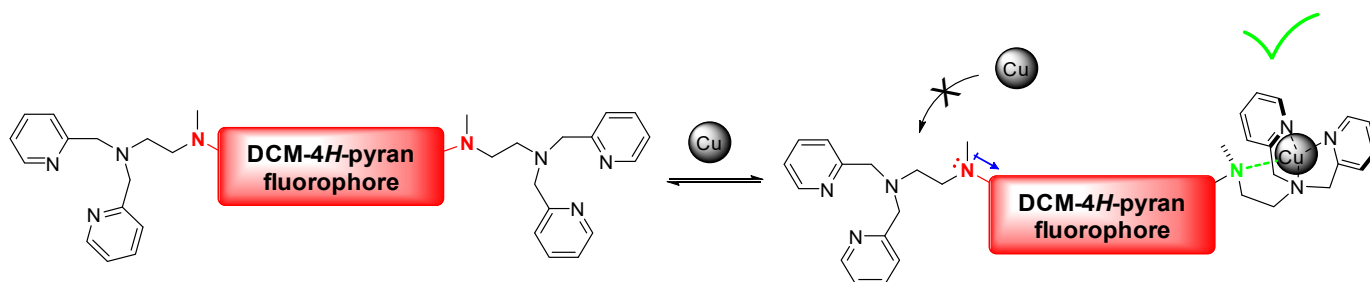


Figure 5. Possible binding mode of copper to **4**. The coordination of the metal includes the nitrogen that is directly coupled to the fluorophore (shown in green), causing a blue-shift in the absorption maximum. The lone pair from the symmetric nitrogen (shown in red) is no longer available for binding a second copper.

Indeed, the experimental data from fluorescence measurements fit well to a 1:1 binding stoichiometry, yielding an association constant of $7.45 \times 10^7 \text{ M}^{-1}$, which is at least one order of magnitude higher when compared to other similar systems [8,10,12–14]. To confirm the stoichiometry, we used the method of continuous variations and obtained the corresponding Job's plot (Figure 6B) [31]. The maximum was observed for a value of 0.52 on the molar fraction of sensor 4, which indicates a 1:1 binding model. The limit of detection [25] for Cu^{2+} was found to be 90.1 nM, which also attests to the high sensitivity of 4 to this metal, even though other systems showed better performance by this parameter (Table 1).

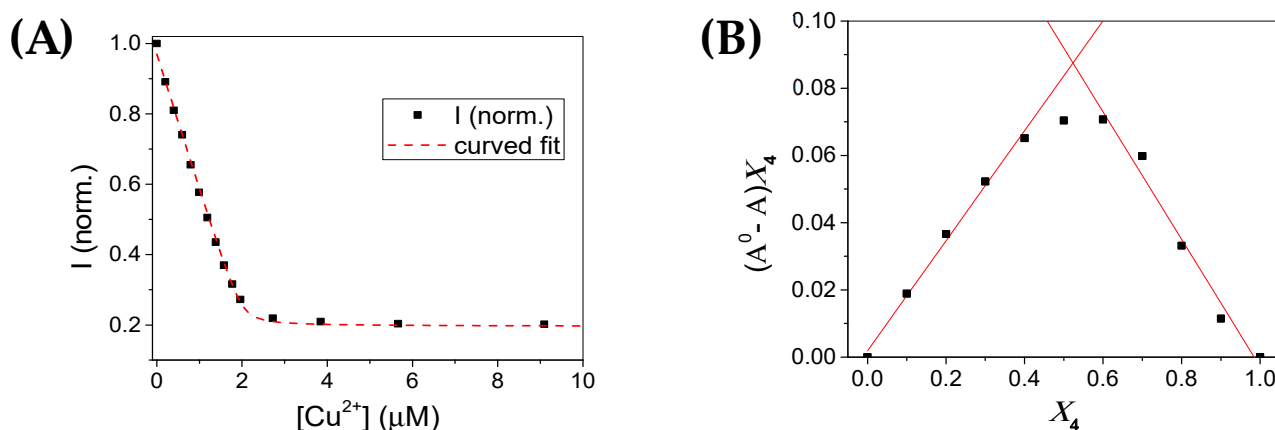


Figure 6. (A) Emission changes of 4 (2.5 μM), in a 50:50 mixture of methanol and 0.01 M HEPES buffer at $\text{pH} = 7.1$ ($\lambda_{\text{EXC}} = 500 \text{ nm}$), in the presence of Cu^{2+} . (B) Job's plot for continuous variation in [4] vs. $[\text{Cu}^{2+}]$. The intersect between the slopes of the linear fits (red lines) was at 0.52 for the molar fraction of 4 (X_4).

The response of 4 to Cu^{2+} in the presence of other metals as interferents was also assessed in a competition assay, where the intensity of the chemosensor was measured primarily in the presence of each metal (2 equivalents), and afterwards upon the addition of one equivalent of copper (II) ions (Figure 7).

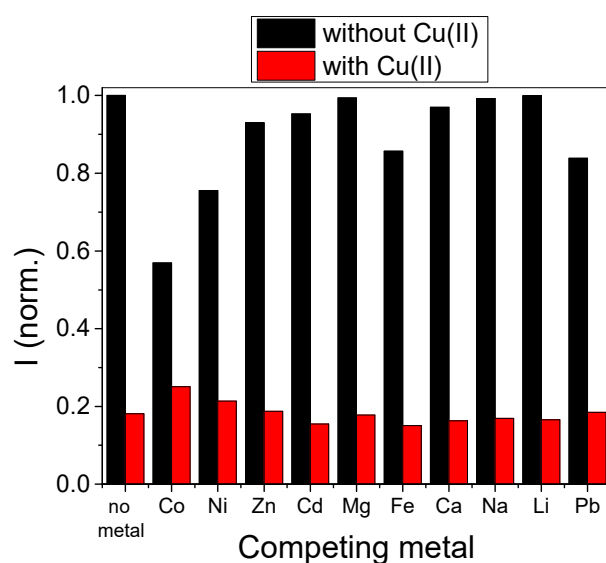


Figure 7. Competition assay illustrating the influences of other metals (2 eqs.) in the detection of one equivalent of Cu^{2+} ions (1 eq.), in a 50:50 mixture of methanol and 0.01 M HEPES buffer at $\text{pH} = 7.1$ ($\lambda_{\text{EXC}} = 500 \text{ nm}$).

Table 1. Comparison between different DPA chemosensors towards copper (II).

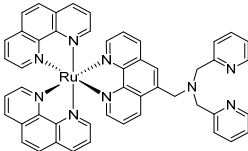
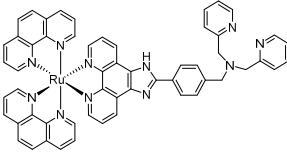
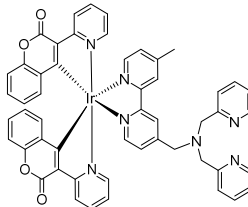
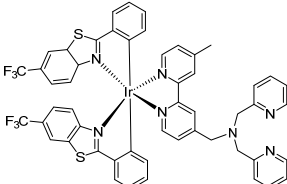
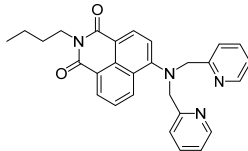
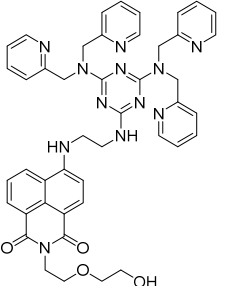
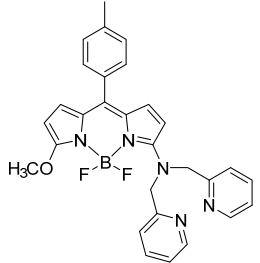
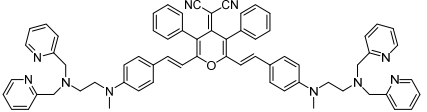
Compound	Conditions/ Solvents	Type of Response	Fluor. QY	Binding Constant	LOD	Ref.
	10 mM HEPES (pH = 7.2)	Luminescent	-	-	155 nM	[7]
	10 mM HEPES (pH = 7.2)	Colorimetric/ luminescent	-	$1.14 \times 10^5 \text{ M}^{-1}$	18.9 nM	[8]
	methanol	Luminescent	0.062 (in CH ₂ Cl ₂)	-	22.3 nM	[9]
	methanol	Luminescent	0.301 (in CH ₂ Cl ₂)	-	11.5 nM	[9]
	Acetonitrile-water (8:2, v/v)	Colorimetric/ luminescent	-	$4.5 \times 10^4 \text{ M}^{-1}$	-	[10]

Table 1. Cont.

Compound	Conditions/ Solvents	Type of Response	Fluor. QY	Binding Constant	LOD	Ref.
	10 mM HEPES (pH = 7.2)	Luminescent	0.190	$3.3 \times 10^5 \text{ M}^{-1}$	2.09 μM	[12]
	acetonitrile	Colorimetric/ luminescent	0.008	$1.28 \times 10^5 \text{ M}^{-1}$	250 nM	[14]
	MeOH-10 mM HEPES (pH = 7.1) (1:1, v/v)	Colorimetric/ luminescent	0.008	$7.45 \times 10^7 \text{ M}^{-1}$	90.1 nM	This work

As can be seen, the metals that interfere the most in the detection of Cu^{2+} are Co^{2+} and Ni^{2+} , which is in agreement with the UV-Vis and emission spectra from Figure 3. For all remaining ions, a clear preference for Cu^{2+} was observed. This result indicates that sample pre-treatment with selective chelators for Co^{2+} (and Ni^{2+}) may be required for copper (II) quantification of aqueous samples that are rich in these two interferent species.

3.4. Paper Test-Strips for Cu^{2+} Detection

As a proof-of-concept, paper test-strips were embedded in concentrated methanolic solutions of chemosensor 4 and air dried, to be used for the detection of copper (II) in aqueous solutions. The paper strips were then subsequently dipped in solutions of different Cu^{2+} concentrations, and immediately left for drying in air. When completely dry, a slight color change was observed from light red to yellow, and the corresponding emission under UV irradiation (365 nm) allowed a clearer image of the quenching effect with increasing concentrations of Cu^{2+} (Figure 8A). Emission spectra from these test-strips were also collected and confirmed a strong decrease in the luminescence of 4 with increasing copper (II) concentration (Figure 8B,C).

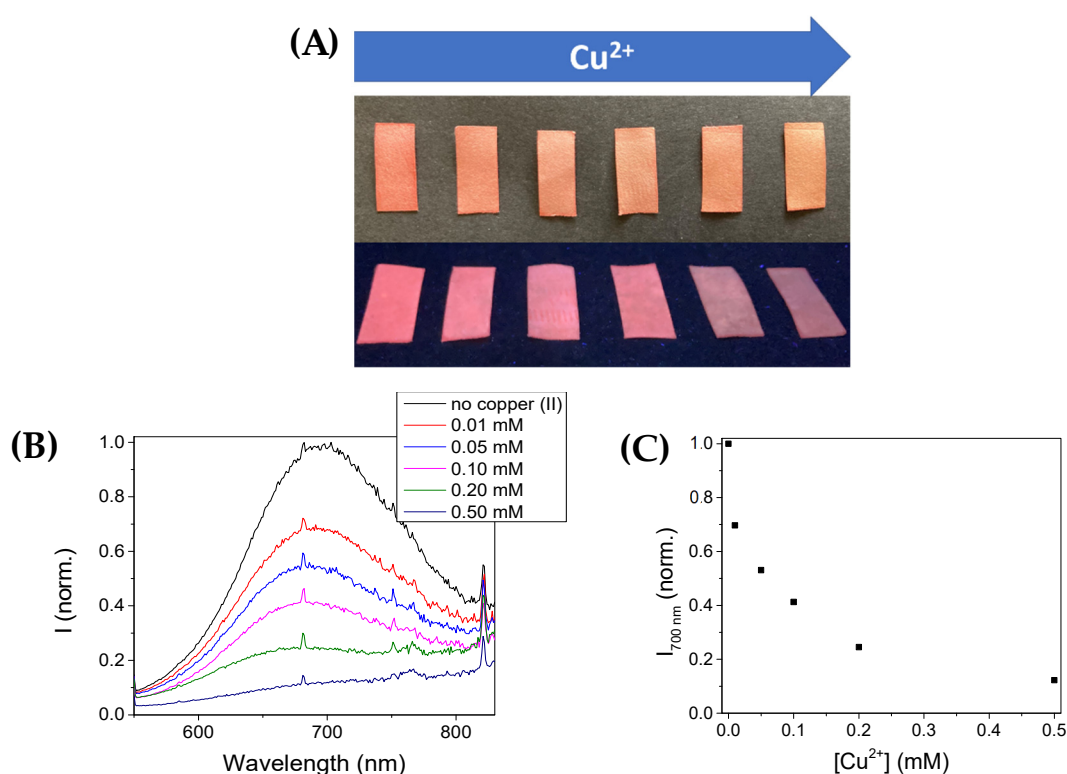


Figure 8. (A) Pictures of paper test-strips with embedded chemosensor 4 upon exposure to increasing copper concentrations (above: under ambient light; below: under 365 nm UV light). (B) Emission spectra from the paper test-strips, and (C) corresponding fluorescence intensity at 700 nm ($\lambda_{\text{EXC}} = 500$ nm).

Overall, the spectra showed lower resolution when compared to chemosensor 4 in solution, though retaining several scattering peaks that were present in all of the prepared paper-strips, which indicates some interference of the matrix in the acquisition of the emission signal. Moreover, the emission maximum was blue-shifted by circa 30 nm. Nevertheless, a clear trend was observed upon increasing copper (II) concentration: a roughly 35% decrease in the fluorescent signal at 0.05 mM and 60% quenching at 0.1 mM. Given the current guidelines from the EU's Environmental Protection Agency (EPA) [32,33], which set the maximum copper concentration to be around 30 μM , these test-strips could potentially

be used as an early screening method for this metal, or ultimately find applications in the detection of aqueous samples with higher copper content, such as waste waters from mining facilities [34].

4. Conclusions

We developed a new donor- π -acceptor DPA-chemosensor system based on a DCM-4H-pyran fluorophore, capable of emitting in the NIR region of the electromagnetic spectrum, and that responds selectively to copper (II) when compared to most of the studied metal ions. In solution, the chemosensor presents a high binding constant with Cu^{2+} , with a limit of detection in the nanomolar range. Paper test-strips embedded with the chemosensor indicated that this system can be used for a rapid screening of copper (II) in drinking water supplies, or waste waters in mining facilities.

Supplementary Materials: The following supporting information can be downloaded at: <https://www.mdpi.com/article/10.3390/chemosensors10080343/s1>. Figures S1–S9: NMR spectra for compounds **1**, **2** and **4**. Figures S10 and S11: HRMS spectra of **4**. Figure S12: pH dependence of fluorescence emission of **4**. Figure S13: Naked-eye changes in solutions of chemosensor **4** with different metal ions. Table S1: Full NMR peak assignment for chemosensor **4**. Table S2: Stokes shift from chemosensor **4** in different organic solvents, and their corresponding empirical polarity parameters.

Author Contributions: Conceptualization, A.J.M.; methodology, A.J.M.; investigation, A.K. and A.J.M.; writing—original draft preparation, A.J.M.; writing—review and editing, A.K.; supervision, A.J.M. All authors have read and agreed to the published version of the manuscript.

Funding: This research was funded by Fundação para a Ciência e Tecnologia, FCT/MCTES, through the Associate Laboratory for Green Chemistry—LAQV (grants UIDB/50006/2020 and UIDP/50006/2020). The NMR spectrometers are part of Rede Nacional de RMN (PTNMR), supported by FCT/MCTES (grant ROTEIRO/0031/2013—PINFRA/22161/2016) (co-financed by FEDER through COMPETE 2020, POCI and PORL and FCT through PIDDAC). A.K. thanks the Erasmus+ Programme of the European Union for a student mobility fellowship.

Institutional Review Board Statement: Not applicable.

Informed Consent Statement: Not applicable.

Data Availability Statement: Not applicable.

Conflicts of Interest: The authors declare no conflict of interest.

References

1. Wu, D.; Sedgwick, A.C.; Gunnlaugsson, T.; Akkaya, E.U.; Yoon, J.; James, T.D. Fluorescent Chemosensors: The Past, Present and Future. *Chem. Soc. Rev.* **2017**, *46*, 7105–7123. [CrossRef]
2. Jeong, Y.; Yoon, J. Recent Progress on Fluorescent Chemosensors for Metal Ions. *Inorg. Chim. Acta* **2012**, *381*, 2–14. [CrossRef]
3. Carter, K.P.; Young, A.M.; Palmer, A.E. Fluorescent Sensors for Measuring Metal Ions in Living Systems. *Chem. Rev.* **2014**, *114*, 4564–4601. [CrossRef]
4. Gerd, M.; Andrea, S.; Lars, H.; Dirk, B.; Thomas, R.; Colin, L.M.; Konrad, B. The Amyloid Precursor Protein of Alzheimer's Disease in the Reduction of Copper (II) to Copper (I). *Science* **1996**, *271*, 1406–1409.
5. Lutsenko, S. Atp7b-/- Mice as a Model for Studies of Wilson's Disease. *Biochem. Soc. Trans.* **2008**, *36*, 1233–1238. [CrossRef] [PubMed]
6. Lee, S.; Liu, Y.; Lim, M.H. Untangling Amyloid- β , Tau, and Metals in Alzheimer's Disease. *ACS Chem. Biol.* **2013**, *8*, 856–865.
7. Liu, X.W.; Xiao, Y.; Zhang, S.B.; Lu, J.L. A Selective Luminescent Sensor for the Detection of Copper (II) Ions Based on a Ruthenium Complex Containing DPA Moiety. *Inorg. Chem. Commun.* **2017**, *84*, 56–58. [CrossRef]
8. Arora, A.; Kaushal, J.; Kumar, A.; Kumar, P.; Kumar, S. Ruthenium(II)-Polypyridyl-Based Sensor Bearing a DPA Unit for Selective Detection of Cu(II) Ion in Aqueous Medium. *ChemistrySelect* **2019**, *4*, 6140–6147. [CrossRef]
9. Yu, T.; Wang, Y.; Zhu, Z.; Li, Y.; Zhao, Y.; Liu, X.; Zhang, H. Two New Phosphorescent Ir(III) Complexes as Efficient Selective Sensors for the Cu^{2+} Ion. *Dye. Pigment.* **2019**, *161*, 252–260. [CrossRef]
10. Wang, H.; Yang, L.; Zhang, W.; Zhou, Y.; Zhao, B.; Li, X. A Colorimetric Probe for Copper(II) Ion Based on 4-Amino-1,8-Naphthalimide. *Inorg. Chim. Acta* **2012**, *381*, 111–116. [CrossRef]
11. Lee, Y.H.; Verwilt, P.; Park, N.; Lee, J.H.; Kim, J.S. Organelle-Selective Di-(2-Picolyl)Amine-Appended Water-Soluble Fluorescent Sensors for Cu(II): Synthesis, Photophysical and in Vitro Studies. *J. Incl. Phenom. Macrocycl. Chem.* **2015**, *82*, 109–116. [CrossRef]

12. Moro, A.J.; Santos, M.; Outis, M.; Mateus, P.; Pereira, P.M. Selective Coordination of Cu^{2+} and Subsequent Anion Detection Based on a Naphthalimide-Triazine(DPA)₂ Chemosensor. *Biosensors* **2020**, *10*, 129. [[CrossRef](#)] [[PubMed](#)]
13. Gomes, L.J.; Moreira, T.; Rodríguez, L.; Moro, A.J. Chalcone-Based Fluorescent Chemosensors as New Tools for Detecting Cu^{2+} Ions. *Dye. Pigment.* **2022**, *197*, 109845. [[CrossRef](#)]
14. Huang, J.; Wang, B.; Ye, J.; Liu, B.; Qiu, H.; Yin, S. A Highly Copper-Selective Ratiometric Fluorescent Sensor Based on BODIPY. *Chin. J. Chem.* **2012**, *30*, 1857–1861. [[CrossRef](#)]
15. Hafuka, A.; Satoh, H.; Yamada, K.; Takahashi, M.; Okabe, S. 3-[Bis(Pyridin-2-Ylmethyl)Amino]-5-(4-Carboxyphenyl)- BODIPY as Ratiometric Fluorescent Sensor for Cu^{2+} . *Materials* **2018**, *11*, 814. [[CrossRef](#)]
16. Sivaraman, G.; Iniya, M.; Anand, T.; Kotla, N.G.; Sunnapu, O.; Singaravadivel, S.; Gulyani, A.; Chellappa, D. Chemically Diverse Small Molecule Fluorescent Chemosensors for Copper Ion. *Coord. Chem. Rev.* **2018**, *357*, 50–104. [[CrossRef](#)]
17. Wang, Y.; Yu, H.; Zhang, Y.; Jia, C.; Ji, M. Development and Application of Several Fluorescent Probes in near Infrared Region. *Dye. Pigment.* **2021**, *190*, 109284. [[CrossRef](#)]
18. Zampetti, A.; Minotto, A.; Cacialli, F. Near-Infrared (NIR) Organic Light-Emitting Diodes (OLEDs): Challenges and Opportunities. *Adv. Funct. Mater.* **2019**, *29*, 1807623. [[CrossRef](#)]
19. Tachapermporn, Y.; Thavornpradit, S.; Charoenpanich, A.; Sirirak, J.; Burgess, K.; Wanichacheva, N. Near-Infrared Aza-BODIPY Fluorescent Probe for Selective Cu^{2+} Detection and Its Potential in Living Cell Imaging. *Dalton Trans.* **2017**, *46*, 16251–16256. [[CrossRef](#)]
20. Huang, X.; Guo, Z.; Zhu, W.; Xie, Y.; Tian, H. A Colorimetric and Fluorescent Turn-on Sensor for Pyrophosphate Anion Based on a Dicyanomethylene-4H-Chromene Framework. *Chem. Commun.* **2008**, 5143–5145. [[CrossRef](#)]
21. Li, H.; Guo, Y.; Li, G.; Xiao, H.; Lei, Y.; Huang, X.; Chen, J.; Wu, H.; Ding, J.; Cheng, Y. Aggregation-Induced Fluorescence Emission Properties of Dicyanomethylene-1,4-Dihydropyridine Derivatives. *J. Phys. Chem. C* **2015**, *119*, 6737–6748. [[CrossRef](#)]
22. Liu, Y.; Lei, Y.; Liu, M.; Li, F.; Xiao, H.; Chen, J.; Huang, X.; Gao, W.; Wu, H.; Cheng, Y. The Effect of: N-Alkyl Chain Length on the Photophysical Properties of Indene-1,3-Dionemethylene-1,4-Dihydropyridine Derivatives. *J. Mater. Chem. C* **2016**, *4*, 5970–5980. [[CrossRef](#)]
23. Xiao, F.; Wang, M.; Lei, Y.; Xie, Y.; Liu, M.; Zhou, Y.; Gao, W.; Huang, X.; Wu, H. An Unexpected 4,5-Diphenyl-2,7-Naphthyridine Derivative with Aggregation-Induced Emission and Mechanofluorochromic Properties Obtained from a 3,5-Diphenyl-4H-Pyran Derivative. *Chem.–Asian J.* **2020**, *15*, 3437–3443. [[CrossRef](#)] [[PubMed](#)]
24. Küster, F.W.; Thiel, A. *Tabelle per le Analisi Chimiche e Chimico-Fisiche*, 14th ed.; Hoepli: Milano, Italy, 1985.
25. McNaught, A.D.; Wilkinson, A. *International Union of Pure Appl. Chem. Compendium of Chemical Terminology*; Blackwell Science: West Sussex, UK, 1997.
26. Drake, J.M.; Lesiecki, M.L.; Camaioni, D.M. Photophysics and Cis-Trans Isomerization of DCM. *Chem. Phys. Lett.* **1985**, *113*, 530–534. [[CrossRef](#)]
27. Thordarson, P. Determining Association Constants from Titration Experiments in Supramolecular Chemistry. *Chem. Soc. Rev.* **2011**, *40*, 1305–1323. [[CrossRef](#)]
28. Reichardt, C.; Harbusch-Görnert, E. Über Pyridinium-N-phenolat-Betaine und ihre Verwendung zur Charakterisierung der Polarität von Lösungsmitteln, X. Erweiterung, Korrektur und Neudefinition der ET-Lösungsmittelpolaritätsskala mit Hilfe eines lipophilen penta-tert-butyl-substituierten Pyridinium-N-phenolat-Betainfarbstoffes. *Liebigs Ann. Chem.* **1983**, *1983*, 721–896. [[CrossRef](#)]
29. Chattopadhyay, N.; Serpa, C.; Pereira, M.M.; Seixas De Melo, J.; Arnaut, L.G.; Formosinho, S.J. Intramolecular Charge Transfer of P-(Dimethylamino)Benzethyne: A Case of Nonfluorescent ICT State. *J. Phys. Chem. A* **2001**, *105*, 10025–10030. [[CrossRef](#)]
30. Moro, A.J.; Cywinski, P.J.; Körsten, S.; Mohr, G.J. An ATP Fluorescent Chemosensor Based on a Zn(II)-Complexed Dipicolylamine Receptor Coupled with a Naphthalimide Chromophore. *Chem. Commun.* **2010**, *46*, 1085–1087. [[CrossRef](#)]
31. Renny, J.S.; Tomasevich, L.L.; Tallmadge, E.H.; Collum, D.B. Method of Continuous Variations: Applications of Job Plots to the Study of Molecular Associations in Organometallic Chemistry. *Angew. Chem. Int. Ed.* **2013**, *52*, 11998–12013. [[CrossRef](#)]
32. Alcock-Earley, B.; Garry, L.; McCarthy, C.; Breslin, C.; Rooney, D. *The Protection of Water Resources: Developing Novel Sensor Materials*; Environmental Protection Agency (EPA): Washington, DC, USA, 2015.
33. Hadži Jordanov, S.; Maletić, M.; Dimitrov, A.; Slavkov, D.; Paunović, P. Waste Waters from Copper Ores Mining/Flotation in 'Bučbim' Mine: Characterization and Remediation. *Desalination* **2007**, *213*, 65–71. [[CrossRef](#)]
34. Santoro, S.; Estay, H.; Avci, A.H.; Pugliese, L.; Ruby-Figueroa, R.; Garcia, A.; Aquino, M.; Nasirov, S.; Straface, S.; Curcio, E. Membrane Technology for a Sustainable Copper Mining Industry: The Chilean Paradigm. *Clean. Eng. Technol.* **2021**, *2*, 100091. [[CrossRef](#)]